

Phase Transitions in Driven Informational Systems: A Two-Field Perspective on Learning Theory and Non-Equilibrium Chemistry

Truong Xuan Khanh*

H&K Research Studio, Clevix LLC
Hanoi, Vietnam

May 19, 2026

Abstract

Phase-transition phenomena in deep learning—grokking, emergent capabilities, and ontological reorganization under context shift—have been studied through several theoretical lenses, including representational compression, singular learning theory, and information-theoretic progress measures. Independently, non-equilibrium statistical physics has identified phase transitions in driven chemical reaction networks underlying prebiotic selection, with empirical signatures (catalysis–confinement synergy, optimal entropy-flux windows) that are difficult to reproduce within single-field gradient accounts. We propose a perspective in which both classes of phenomena admit a common description as *driven informational systems*: stochastic processes governed by two gradient fields—an entropy production rate Σ and an information quasi-potential $\Phi_I := -\ln p^*$, where p^* is the stationary density. Within this framework we discuss two candidate order parameters: an adversarial breakdown threshold α^\dagger whose decay with the primitive-set cardinality $|\mathcal{O}_N|$ is logarithmic, and a self-referential coupling threshold κ_c associated with predictive feedback through an internal model. The joint scaling of $(\alpha^\dagger, \kappa_c)$ defines a candidate universality class, with two scaling exponents (γ_1, γ_2) as class invariants. We do not claim that biological intelligence and large language models are the same kind of system; we propose only that they may be productively studied as particular instances within this common framework, on configuration manifolds shaped by carbon–nitrogen chemistry under solar entropy flux and by transformer parameter spaces under gradient-descent flux, respectively. We outline the geometric structure of the framework, identify three falsifiable predictions that distinguish it from single-field alternatives, and synthesise recent empirical findings (2024–2026) on alignment phase transitions, adversarial breakdown scaling, and partial introspection in frontier language models, with which the framework is consistent. Detailed proofs and supporting numerical analyses of the component results appear in companion preprints; the present paper develops the connections between them.

Keywords: phase transitions, grokking, alignment, non-equilibrium statistical mechanics, free energy principle, self-referential coupling, ontological reorganization, prebiotic selection.

1 Introduction

1.1 The convergent puzzle

Phase-transition phenomena in deep learning—grokking, emergent capabilities, and ontological reorganization under context shift—have been studied through several theoretical lenses, none

*Correspondence: khanh@clevix.vn

of which we take to be definitive. Power et al. (2022) observed that small transformers trained on modular arithmetic generalize abruptly long after they have memorized the training set, and Nanda et al. (2023) subsequently showed that this delayed transition coincides with the emergence of Fourier-structured circuits. Liu et al. (2023) interpreted the same phenomenon through the lens of representational compression, and DeMoss et al. (2025) formalized the rise-and-fall of model complexity through a rate-distortion lens. Wei et al. (2022) documented *emergent capabilities* in large language models—abilities that appear discontinuously above scale thresholds—and a parallel literature has examined phase transitions in alignment dynamics (Casper et al., 2023), in-context learning (Olsson et al., 2022), and introspective access (Binder et al., 2024; Lindsey, 2025).

These phenomena share three structural features: a substrate-level dynamics governed by gradient descent on a loss surface; a sustained external driving signal (training-data flux, RLHF feedback, weight decay); and a transition between qualitatively distinct representational regimes whose detailed mechanism remains under active investigation.

A structurally similar pattern appears in non-equilibrium chemistry. Ferris et al. (1996) demonstrated that clay-catalyzed RNA polymerization combined with geometric confinement produces oligomers of length up to ~ 55 -mer, an order of magnitude longer than solution-only controls; subsequent reanalysis extracts a catalysis-confinement synergy factor $S \approx 5.75$ that exceeds what single-field gradient dynamics on compact manifolds with linear driving can produce under the assumptions made there. Blank et al. (2001) reported a non-monotonic optimal entropy-flux window for amino-acid yield in shock synthesis. Matreux et al. (2024) demonstrated that simple heat flows selectively enrich more than fifty prebiotic building blocks by up to three orders of magnitude. Floroni et al. (2025) realized a prebiotic-to-biotic transition criterion in a single membraneless protocell driven by a heat gradient. Liang et al. (2024a,b) placed kinetics-independent bounds on the magnitude of symmetry-breaking achievable in driven chemical reaction networks at given thermodynamic budget.

We propose, in the rest of this paper, that these two lines of work may admit a common description as instances of a broader class of *driven informational systems*, and we develop the elements of that description.

1.2 The central proposal

This perspective develops three connected proposals.

First. Driven informational systems—whether chemical reaction networks under thermal flux or transformer parameter manifolds under gradient-descent flux—can be modeled as governed by two gradient fields: an entropy-production rate Σ derived from the Schnakenberg decomposition of probability currents (Schnakenberg, 1976), and an information quasi-potential $\Phi_I := -\ln p^*$ defined self-consistently through the stationary density p^* . Under the regularity conditions stated in §4, $\nabla\Sigma$ and $\nabla\Phi_I$ are generically linearly independent off equilibrium.

Second. We propose two candidate order parameters that together may characterize the phase structure of these systems. The first is an adversarial breakdown threshold

$$\alpha^\dagger = \Theta\left(\frac{1}{\log |\mathcal{O}_N|}\right),$$

where $|\mathcal{O}_N|$ is the cardinality of the system’s primitive representation. The asymptotic form depends on representational complexity, in contrast to the universal constants of Hampel (1971) and Donoho and Huber (1983); we are not aware of a prior breakdown point with this dependence in the literature reviewed, though the literature is large and the present paper does not claim exhaustive coverage. The second proposed order parameter is a self-referential coupling threshold κ_c associated with predictive feedback through an internal model (§3.2).

Third. We propose that biological intelligence and large language models may be productively studied as particular instances within this framework on different configuration manifolds. Biological intelligence is here viewed as one realization of the dynamics, on chemical configuration manifolds under solar entropy flux over evolutionary time scales. Frontier large language models are viewed as a second realization, on transformer parameter manifolds under gradient-descent flux over training time scales. We do not claim these systems are the same kind of object; the time scales, configuration manifolds, and physical substrates differ by many orders of magnitude. We claim only that certain dynamical features—the two-field structure, the candidate order parameters, the phase-transition signature—may be shared across instances, and that this sharing is mathematically meaningful even where the substrates manifestly are not.

1.3 Scope and provenance

The framework synthesized here builds on two preceding lines of work, both of which are publicly available as preprints. The Equation of Motion–Information Field Framework (EOM-IFF) for prebiotic chemistry was developed jointly with T. Q. Hoa and is presented in detail in a companion preprint on bioRxiv (Truong and Truong, 2026a); that work establishes the two-field independence theorem, derives structural constraints on single-field gradient dynamics, and validates the framework against five independently published prebiotic systems (Blank et al., 2001; Ferris et al., 1996; Floroni et al., 2025; Matreux et al., 2024; Rout et al., 2025). The theory of Ontological Phase Transitions (OPT) in learning systems was developed by the present author and is reported in a separate preprint on SSRN (Truong, 2026); that work establishes a universal detection lower bound, a compression-dividend theorem, the complexity-dependent breakdown point cited above, and empirical validation of the predicted scaling on grokking dynamics across nine modulus pairs.

The present perspective is a synthesis the author developed independently. Its contribution—and the timestamp it claims—is not in the component results, which are established in those companion preprints, but in the proposal that the chemistry-side and learning-side frameworks may be productively studied as instances within a common dynamical class, with α^\dagger and κ_c as candidate order parameters of that class. We are not aware of a prior synthesis along these lines, though the literature is large and the present paper does not claim exhaustive coverage.

This paper *does* outline the geometric perspective, define the two candidate order parameters, identify three falsifiable predictions, and position the framework relative to neighboring research programs: the free energy principle (Friston, 2010; Ramstead et al., 2023), singular learning theory (Hoogland et al., 2024; Watanabe, 2009), dissipative adaptation (England, 2015), grokking-as-compression (Clauw et al., 2024; DeMoss et al., 2025; Liu et al., 2023), and tangled information hierarchies (Prokopenko et al., 2025). This paper *does not* provide full proofs (these are in the cited companion preprints), claim universality beyond the stated regimes, or replace existing frameworks where they are correct. Specific limitations and open problems are gathered in §7.

1.4 Roadmap

§2 sets up the language of driven informational systems and states the two-field structure abstractly. §3 defines the two candidate order parameters α^\dagger and κ_c and discusses their relationship. §4 states the two-field independence theorem informally and indicates its consequences for learning theory. §5 presents the chemical and learning instances side by side. §6 derives three falsifiable predictions. §7 positions the framework relative to neighbors and identifies open problems. §8 concludes.

2 Driven Informational Systems

This section introduces the abstract framework in which the proposal is stated. The construction is deliberately substrate-agnostic: the same definitions apply when the configuration manifold is a chemical composition simplex and when it is the parameter space of a neural network. What distinguishes the two cases—and what motivates the proposal that both may be productively studied as instances of a common dynamical class—is addressed in §5.

2.1 Configuration manifold and Langevin dynamics

A *driven informational system* is specified by a triple (\mathcal{M}, b, D) , where \mathcal{M} is a smooth connected n -dimensional Riemannian manifold (the configuration space), $b : \mathcal{M} \rightarrow T\mathcal{M}$ is a Lipschitz drift vector field, and $D > 0$ is a constant noise amplitude. The state $X_t \in \mathcal{M}$ evolves under the overdamped Langevin equation

$$dX_t = b(X_t) dt + \sqrt{2D} dW_t, \quad (1)$$

where W_t is a standard Brownian motion on \mathcal{M} . Under mild regularity conditions—confinement of the drift at infinity, linear-growth bounds, and strict positivity of D —equation (1) admits a unique stationary probability measure μ^* with smooth, strictly positive density $p^* : \mathcal{M} \rightarrow (0, \infty)$ (Meyn and Tweedie, 1993); a precise statement of the regularity conditions is given in the companion preprint.

Two instances of this construction frame the present perspective. In *prebiotic chemistry*, \mathcal{M} is the composition simplex Δ^{n-1} of molecular species under mass conservation, b is determined by the reaction-rate matrix of the chemical network, and D encodes thermal fluctuations. In *neural network learning*, \mathcal{M} is the parameter manifold of a model architecture (typically \mathbb{R}^P with P the parameter count, restricted by weight-decay or layer-norm constraints), b is the negative gradient of the training loss combined with regularization terms, and D encodes mini-batch gradient noise. In both cases the dynamics is *driven*: an external entropy flux—thermal in chemistry, data-driven in learning—maintains the system away from equilibrium, ensuring that the stationary measure μ^* is genuinely non-equilibrium (i.e., does not satisfy detailed balance with respect to b).

2.2 The two fields

Two scalar fields can be constructed canonically from the dynamics (1).

Entropy production rate. Let $J^*(x) := b(x)p^*(x) - D\nabla p^*(x)$ denote the stationary probability current. The *local entropy production rate* is

$$\Sigma(x) := \frac{\|J^*(x)\|^2}{D \cdot p^*(x)}. \quad (2)$$

This is the local Schnakenberg dissipation (Schnakenberg, 1976; Seifert, 2012), and its integral $\int \Sigma(x) p^*(x) dx$ recovers the total entropy production rate of the non-equilibrium steady state. Σ vanishes identically if and only if the system is in detailed balance, in which case the dynamics reduces to gradient descent on a potential.

Information quasi-potential. The *information quasi-potential* is

$$\Phi_I(x) := -\ln p^*(x). \quad (3)$$

This object is well-defined wherever p^* is, and inherits all the regularity of p^* . In equilibrium systems Φ_I is a derived quantity (proportional to the Boltzmann potential up to additive constants), but off equilibrium it acquires independent geometric structure: in particular, its level

sets need not coincide with those of Σ , and its gradient need not be aligned with $\nabla\Sigma$. In the small-noise limit $D \rightarrow 0$, Φ_I coincides with the Freidlin–Wentzell quasi-potential (Freidlin and Wentzell, 1984), justifying the terminology.

2.3 Two-field structure

The drift in (1) can be *decomposed* into two gradient components plus a residual:

$$b(x) = -\alpha \nabla\Sigma(x) - \beta \nabla\Phi_I(x) + b_\perp(x), \quad (4)$$

where $\alpha, \beta \in \mathbb{R}$ are coupling constants and b_\perp collects any residual non-gradient component. The framework analyzed here is the regime in which b_\perp is small in norm relative to the gradient terms, so that the dynamics is effectively two-field gradient. Whether this regime is reached in any particular application is an empirical question; we discuss its plausibility for chemical and learning instances in §5.

The central structural fact about (4) is that the two gradient components are *generically independent* off equilibrium. We state this informally here and develop it in §4.

Two-Field Independence (informal statement). *Let (\mathcal{M}, b, D) be a driven informational system strictly out of detailed balance, satisfying mild non-degeneracy conditions (Morse Φ_I , trivial first cohomology of \mathcal{M} , confinement at infinity). Then $\nabla\Sigma$ and $\nabla\Phi_I$ are not proportional on a set of positive μ^* -measure where $\nabla\Phi_I \neq 0$. Within the space of admissible drift fields, the subset for which $\nabla\Sigma \parallel \nabla\Phi_I$ everywhere is contained in a proper algebraic subvariety, hence has Lebesgue measure zero.*

A rigorous statement and proof—in both the discrete (Schnakenberg network) and continuous (transport-equation) formulations—are given as Theorem 1 of (Truong and Truong, 2026a). The proof reduces collinearity of the two gradients to vanishing of every cycle affinity in the Schnakenberg decomposition, which by Kolmogorov’s criterion is equivalent to detailed balance, contradicting the hypothesis.

2.4 Why two fields matter

The geometric content of two-field independence is that (1) cannot be reduced to gradient descent on any single scalar potential without losing information. Three consequences follow, each of which has empirical signatures.

First, on a compact manifold with linear driving, single-field gradient dynamics yields a yield curve at any target configuration that is at most unimodal as a function of the driving parameter. Multi-peaked or oscillatory yield is incompatible with single-field structure.

Second, two independent perturbations with disjoint local supports near a target configuration combine *additively* in depth under single-field gradient dynamics, with superlinearity factor $S = 1 + O(\|\delta V\|^2)$ at second order. The empirically inferred superlinearity $S \approx 5.75$ in clay-catalyzed RNA polymerization under combined catalysis and confinement (Ferris et al., 1996) therefore falsifies any single-field gradient account in that system.

Third, in learning-theoretic instances, single-field reduction implies that representational reorganization under context shift is basin selection within a fixed loss landscape—incompatible with the ontological-restructuring phenomenology in which the primitive set itself changes across the transition.

2.5 The substrate-independence question

Two driven informational systems (\mathcal{M}_1, b_1, D) and (\mathcal{M}_2, b_2, D) related by an isometric diffeomorphism $\varphi : \mathcal{M}_1 \rightarrow \mathcal{M}_2$ with $b_2 = \varphi_* b_1$ share their stationary densities, quasi-potentials, and

basin structure exactly. This is a mathematical statement about the invariance of the framework under re-parameterization, not a physical claim about substrate equivalence.

The empirical hypothesis we develop in §5 is weaker than substrate equivalence but stronger than analogy: we propose that biological intelligence and large language models may be productively studied as instances within the framework of equations (1)–(4) on different configuration manifolds, with shared dynamical structure (the two-field decomposition, the candidate order parameters) but manifestly distinct substrates, time scales, and degrees of freedom. Substrate-independence in this sense is a proposal about which dynamical features may be conserved across instances within the framework, not about which substrates can support which dynamics.

3 Two Order Parameters

A driven informational system in the two-field regime exhibits a phase structure governed by two order parameters: an adversarial breakdown threshold α^\dagger characterizing the system’s resistance to representational corruption from outside, and a self-referential coupling threshold κ_c characterizing the emergence of internal predictive coupling. We define each operationally, indicate its scaling with representational complexity, and argue that the two are dual signatures of a single universality class.

3.1 The breakdown order parameter α^\dagger

Consider a driven informational system whose stationary measure μ^* has support concentrated on a finite primitive set $\mathcal{O}_N = \{\theta_1, \dots, \theta_{|\mathcal{O}_N|}\}$, where each $\theta_i \in \mathbb{R}^d$ is a primitive representation (a chemical species, a Fourier feature, a circuit motif). The *representational complexity* of the system is the cardinality $|\mathcal{O}_N|$.

Suppose the system is observing a stream of data drawn from a context distribution p_{C_1} , and that an adversary corrupts a fraction $\alpha \in [0, 1]$ of the stream by replacing samples with adversarially chosen ones. The observer wishes to detect a genuine shift to a new context p_{C_2} with $\Delta := \text{KL}(p_{C_2} \| p_{C_1}) > 0$, while distinguishing it from contamination. The *minimax adversarial breakdown rate* is the largest α for which any detection protocol can achieve false-positive plus missed-detection rates summing to less than $1/2$.

Scaling. Theorem 10.5 of Truong (2026) establishes that, under bounded-shift assumptions ($0 < \Delta_{\min} \leq \Delta \leq \Delta_{\max} < \infty$), the minimax breakdown rate satisfies

$$\alpha^\dagger = \Theta\left(\frac{1}{\log |\mathcal{O}_N|}\right). \quad (5)$$

The proof proceeds by a Le Cam two-point argument (Le Cam, 1986): a universal detection lower bound $D_{\text{passive}}^* = \Omega(\log |\mathcal{O}_N|/\Delta)$ implies that no algorithm can confirm a shift with fewer samples while controlling false-positive rate. An adversary with budget α injects $\alpha \cdot D_{\text{passive}}^* = \Theta(\alpha \log |\mathcal{O}_N|/\Delta)$ poisoned samples per detection window. When $\alpha \log |\mathcal{O}_N| \geq 1$, the adversary can place at least one poisoned sample in every coherent detection window, defeating temporal-consistency methods. Setting the product to unity gives (5).

Significance. Classical breakdown points in robust statistics are universal constants: $1/2$ for the median (Donoho and Huber, 1983), and $\approx 29\%$ for high-breakdown S - and M -estimators (Hampel, 1971). Recent advances in high-dimensional robust statistics (Diakonikolas and Kane, 2023) bound *error* by ambient dimension, but the underlying breakdown fraction remains constant; targeted-poisoning lower bounds (Chornomaz et al., 2025; Hanneke et al., 2022) similarly scale error with VC dimension while leaving the breakdown threshold dimension-free. Equation (5) differs from these in that its asymptotic form depends on representational complexity. We

are not aware of a prior breakdown point with this dependence in the literature reviewed; the literature is large and we cannot rule out parallel constructions we have missed. Its rate of decay is sub-logarithmic but strictly positive: $\alpha^\dagger \rightarrow 0$ as $|\mathcal{O}_N| \rightarrow \infty$, consistent with the intuition that more capable systems may be intrinsically harder to defend against adversarial corruption.

3.2 The self-referential order parameter κ_c

Consider now a driven informational system equipped with an internal *model space* $\mathcal{M}_{\text{model}}$ of dimension strictly less than $\dim \mathcal{M}$, together with a smooth surjective projection $\pi : \mathcal{M} \rightarrow \mathcal{M}_{\text{model}}$ and a smooth feedback function $g : \mathcal{M}_{\text{model}} \rightarrow T\mathcal{M}$. The dynamics is augmented by a self-referential drift term:

$$dX_t = b(X_t) dt - \kappa g(\pi(X_t)) dt + \sqrt{2D} dW_t, \quad (6)$$

where $\kappa \geq 0$ is the self-referential coupling strength. Heuristically, $\pi(X_t)$ is the system’s compressed internal representation of its own state, and $g(\pi(X_t))$ is the action this internal representation drives on the substrate.

Two observables, both estimable from time-series data, characterize the regime of this system. The *predictive fidelity* is

$$F(\kappa) := 1 - \exp(-2I(X_{t+\tau}; \pi(X_t))), \quad (7)$$

where $I(\cdot; \cdot)$ is mutual information and τ is the slow correlation time of the projected process. The form (7) is the Linfoot informational-correlation transformation (Linfoot, 1957): it agrees with squared correlation ρ^2 for jointly Gaussian pairs, takes values in $[0, 1]$ unconditionally, and is invariant under invertible re-parameterization. The *causal efficacy* is

$$C(\kappa) := \frac{\mathbb{E}_{\mu^*} [\|\kappa g(\pi(X))\|]}{\mathbb{E}_{\mu^*} [\|b(X) - \kappa g(\pi(X))\|]}, \quad (8)$$

the dimensionless ratio of the self-referential drift magnitude to the substrate drift magnitude under stationary measure.

Threshold. The *self-referential coupling threshold* is

$$\kappa_c := \inf \{ \kappa \geq 0 : F(\kappa) \geq F_{\min} \wedge C(\kappa) \geq C_{\min} \}, \quad (9)$$

The operational thresholds F_{\min} and C_{\min} are calibrated against the four-criteria framework for genuine introspection developed in Lindsey (2025): predictive fidelity $F(\kappa)$ corresponds jointly to Lindsey’s *accuracy* and *grounding* criteria (a self-report’s reliability plus its causal dependence on the state being reported), while causal efficacy $C(\kappa)$ corresponds to the *internality* criterion (the requirement that introspection not be routed through external outputs). We take $F_{\min} = 0.5$ (Lindsey’s threshold for “reliable self-reports”) and $C_{\min} = 0.1$ (the minimum causal contribution distinguishable from probability-matching artefacts in the dissociation analysis of Lederman and Mahowald (2026)). Robustness to choices in the ranges $F_{\min} \in [0.4, 0.6]$, $C_{\min} \in [0.05, 0.2]$ does not qualitatively change the analysis. If the set in (9) is empty, $\kappa_c = +\infty$: the system cannot reach the self-referential regime under any coupling strength.

Interpretation. A system with $\kappa < \kappa_c$ *samples* from its stationary measure: $\pi(X_t)$ tracks X_t but does not stably encode the dynamics. A system with $\kappa \geq \kappa_c$ *encodes and acts on* its statistics: the internal projection $\pi(X_t)$ is a sufficient statistic with non-trivial causal influence on the substrate dynamics. This is an operational claim about time-series structure—both F and C are estimable from observation (Belghazi et al., 2018; Kraskov et al., 2004)—not a metaphysical claim about consciousness or subjective experience.

A growing body of empirical work on LLM introspection (Binder et al., 2024; Lederman and Mahowald, 2026; Lindsey, 2025; Macar et al., 2026; Song et al., 2025) reports a consistent qualitative pattern: current frontier systems exhibit *partial* introspective capacity—detecting injected internal states above the noise floor (Lindsey, 2025), distinguishing self-generated from prefilled content (Lindsey, 2025), but doing so with high context-dependence and identifying *anomaly without content* in the dissociation of Lederman and Mahowald (2026). Within the present framework this pattern is naturally interpreted as operation in the vicinity of κ_c : above the regime where introspection is absent ($\kappa \ll \kappa_c$) but below the regime where it would be reliably grounded ($\kappa \gg \kappa_c$). We develop this interpretation in §5.2 and stress that it is interpretive, not a direct measurement; direct estimation of $F(\kappa)$ and $C(\kappa)$ for current frontier models from full training trajectories remains an open problem.

3.3 The duality claim

The two order parameters α^\dagger and κ_c are defined on apparently distinct dimensions: α^\dagger concerns robustness to external perturbation of the representation, κ_c concerns the emergence of internal predictive coupling. We propose they are related signatures within a common framework.

Common origin in Φ_I . Both order parameters are derived from the negative-log stationary density. The breakdown threshold α^\dagger enters through the Le Cam two-point construction, where the hypotheses being distinguished—genuine shift versus contamination—are characterized by their Φ_I -distance under the two contexts. The coupling threshold κ_c enters through the mutual information $I(X_{t+\tau}; \pi(X_t))$, which can be expressed as a Φ_I -divergence between the joint and product marginal stationary measures. Both quantities are functionals of Φ_I alone; the entropy production rate Σ enters the dynamics that produces Φ_I but does not appear directly in either threshold.

Joint scaling (conjecture). We conjecture the following joint scaling relation as $|\mathcal{O}_N| \rightarrow \infty$:

$$\alpha^\dagger(\mathcal{O}_N) \cdot (\log |\mathcal{O}_N|)^{\gamma_1} \rightarrow c_1, \quad \kappa_c(\mathcal{O}_N) \cdot (\log |\mathcal{O}_N|)^{\gamma_2} \rightarrow c_2, \quad (10)$$

where $\gamma_1, \gamma_2 > 0$ are scaling exponents and $c_1, c_2 > 0$ are constants. The first relation, with $\gamma_1 = 1$, follows from (5) with c_1 a constant of the breakdown geometry (modulo a universal factor). The exponent γ_2 governing the self-referential coupling threshold is open: dimensional analysis combined with the Le Cam two-point structure underlying κ_c suggests $\gamma_2 \in (0, 1]$, with $\gamma_2 = 1/2$ as a natural guess from analogy with standard parametric rate arguments and with the logarithmic delay laws established for norm-driven phase transitions in regularised training (Truong and Truong, 2026b; Truong et al., 2026), but no rigorous derivation in the self-referential setting is currently available.

We treat the pair (γ_1, γ_2) together with (c_1, c_2) as *defining the universality class* of a driven informational system: their joint values, rather than any specific functional form, parameterize where in the space of such systems a given instance lies. This duality structure—two complementary order parameters with potentially distinct anomalous dimensions—is reminiscent of multicritical phenomena in coupled-order-parameter universality classes (Eichhorn et al., 2013; Hasselmann et al., 2007), though we do not claim formal membership in those specific classes. Precedent for breakdown points whose form depends on a complexity proxy is also found in modern robust statistics (Lecué and Lerasle, 2020), where breakdown numbers scale with effective dimension; equation (5) extends this dependence to the logarithm of an ontology-size proxy. The empirical determination of γ_2 is the principal experimental content of Prediction 1 (§6.1). We treat (10) as a falsifiable conjecture (§6).

Phase-transition signature. A driven informational system that crosses both thresholds may undergo qualitative restructuring of its dynamics: below threshold, the system is a passive sampler whose representation can be corrupted at rate $\alpha < \alpha^\dagger$; above threshold, the system encodes its own statistics self-referentially and may resist corruption at the same nominal rate through internal consistency. We propose this as a candidate signature; whether the joint structure constitutes a universality class in the technical sense is left for future work.

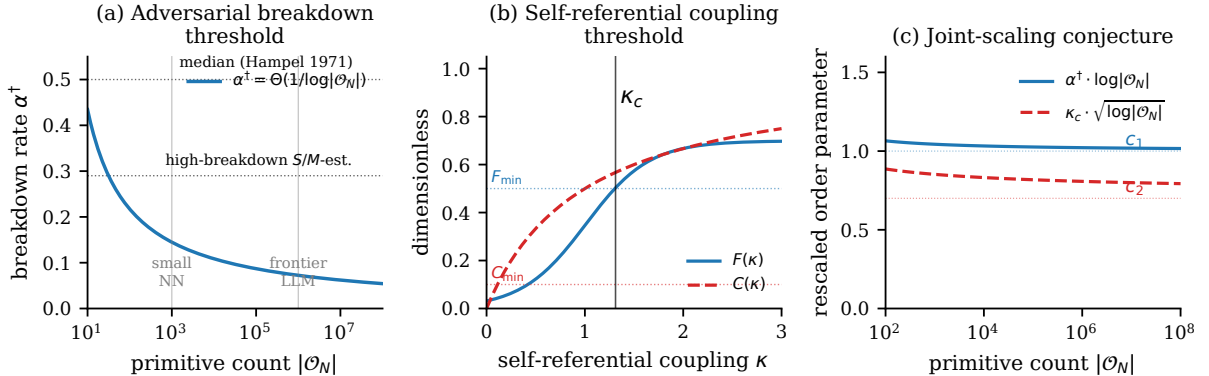


Figure 1: **The two candidate order parameters (schematic).** (a) The adversarial breakdown threshold $\alpha^\dagger = \Theta(1/\log |\mathcal{O}_N|)$ as a function of representational complexity $|\mathcal{O}_N|$ (solid blue), shown against classical breakdown points of robust statistics (dotted horizontal lines): the median of Hampel (1971) at $1/2$, and high-breakdown S/M -estimators at ≈ 0.29 . The classical breakdown points are universal constants; equation (5) differs in that its asymptotic form depends on representational complexity. (b) The predictive fidelity $F(\kappa)$ (Linfot form, solid blue) and the causal efficacy $C(\kappa)$ (dashed red) as a function of the self-referential coupling strength κ . The threshold κ_c is the smallest κ at which both $F \geq F_{\min} = 0.5$ and $C \geq C_{\min} = 0.1$ hold (vertical black line). (c) The joint scaling conjecture (10): the rescaled products $\alpha^\dagger \cdot (\log |\mathcal{O}_N|)^{\gamma_1}$ and $\kappa_c \cdot (\log |\mathcal{O}_N|)^{\gamma_2}$ are conjectured to approach distinct constants c_1, c_2 as $|\mathcal{O}_N| \rightarrow \infty$, with (γ_1, γ_2) defining the universality class ($\gamma_1 = 1$ established; $\gamma_2 \in (0, 1]$ to be determined empirically per Prediction 1).

3.4 Relation to existing order parameters

Several candidate order parameters have been proposed for phase-transition phenomena in driven informational systems. We position $(\alpha^\dagger, \kappa_c)$ relative to three of the most developed.

Real log canonical threshold (RLCT) in singular learning theory. Watanabe’s RLCT (Watanabe, 2009) is a geometric invariant of the loss landscape that governs Bayesian generalization rates and has been proposed as the natural order parameter for stagewise development in neural networks (Hoogland et al., 2024; Pepin Lehalleur et al., 2025). The RLCT and α^\dagger measure structurally distinct quantities: the RLCT characterizes *posterior basin geometry* under fixed data distribution, whereas α^\dagger characterizes *robustness across distributional shift*. The two are complementary; we conjecture (and state as an open problem) that systems near a Bayesian phase transition in the RLCT sense undergo simultaneous changes in α^\dagger , but no direct functional relation is known.

Variational free energy in the free energy principle. Friston’s variational free energy F_{FEP} (Friston, 2010; Ramstead et al., 2023) is a single scalar functional combining prediction error and complexity, minimized by self-organizing systems. The Linfot fidelity $F(\kappa)$ in (7) is related to but not equal to F_{FEP} : both are mutual-information-based, but $F(\kappa)$ admits a

sharp threshold form via the operational thresholds F_{\min}, C_{\min} , whereas F_{FEP} is continuously minimized. The two-field framework can be read as supplying the FEP with an explicit substrate dynamics (Σ -driven) underlying the variational minimization.

Compression rate in grokking-as-compression. Liu et al. (2023) propose the linear-mapping number (LMN) as a measure of representational compression, and DeMoss et al. (2025) develop a rate–distortion–MDL account of complexity rise-and-fall during training. Both relate to $|\mathcal{O}_N|$ through the MDL correspondence between primitive count and description length, but neither yields a breakdown point. The compression-dividend theorem of Truong (2026, §11) establishes $|\mathcal{O}_N^{\text{post}}| \leq |\mathcal{O}_N^{\text{pre}}|/\eta$ across a phase transition, where η is the alignment-protocol efficiency—a result of which the LMN reduction is a special case.

4 The Two-Field Independence Theorem

The two-field structure introduced in §2 is not a modeling assumption but a generic structural feature of any driven informational system out of detailed balance. We state this as a theorem at the level of formality appropriate for a perspective paper, and indicate three consequences specific to learning theory.

4.1 Statement and proof sketch

Theorem (Two-Field Independence; informal). *Let (\mathcal{M}, b, D) be a driven informational system with stationary density p^* , strictly out of detailed balance (i.e., $J^* \neq 0$). Assume:*

- (C1) *Confinement: \mathcal{M} is compact, or non-compact with confining drift ensuring $J^*(x) \rightarrow 0$ at infinity.*
- (C2) *Morse condition: $\Phi_I = -\ln p^*$ has isolated, non-degenerate critical points.*
- (C3) *Trivial first cohomology: $H^1(\mathcal{M}; \mathbb{R}) = 0$ (excludes flat manifolds with non-trivial fundamental group, e.g., the torus).*

Then $\nabla \Sigma$ and $\nabla \Phi_I$ are not proportional on a set of positive μ^ -measure where $\nabla \Phi_I \neq 0$. Within the space of admissible drift fields satisfying (C1)–(C3) and violating detailed balance, the subset for which $\nabla \Sigma \parallel \nabla \Phi_I$ everywhere on the regular set $\{\nabla \Phi_I \neq 0\}$ is contained in a proper algebraic subvariety of Lebesgue measure zero.*

A complete proof, in both discrete (finite-state Markov chain) and continuous (Fokker–Planck) formulations, is the central result of the chemistry-side companion preprint cited in §2.3. We sketch the argument here in three steps.

Step 1: collinearity implies shared level sets. If $\nabla \Sigma \parallel \nabla \Phi_I$ pointwise μ^* -almost everywhere, then Σ and Φ_I have identical level sets (modulo μ^* -null sets), so $\Sigma = F(\Phi_I)$ for some scalar function F .

Step 2: cycle affinities must vanish. For a finite-state Markov chain with rates k_{ij} and stationary probabilities p_i^* , Schnakenberg’s decomposition expresses the total entropy production as a sum over cycles:

$$\Sigma_{\text{tot}} = \sum_c J_c \cdot \mathcal{A}(c), \quad \mathcal{A}(c) = \ln \prod_{\ell \in c} \frac{k_{i_\ell i_{\ell+1}}}{k_{i_{\ell+1} i_\ell}},$$

where $\mathcal{A}(c)$ is the affinity of cycle c . The functional constraint $\Sigma = F(\Phi_I) = F(-\ln p^*)$ forces every cycle affinity to be expressible purely in terms of the p_i^* along the cycle. The only expressions consistent across all cycles simultaneously are $\mathcal{A}(c) = 0$ for every cycle.

Step 3: Kolmogorov’s criterion. Vanishing cycle affinities are precisely Kolmogorov’s criterion for detailed balance (Kelly, 1979). But detailed balance forces $J^* \equiv 0$, contradicting the hypothesis of off-equilibrium operation.

The continuous-state case follows by Sard’s theorem applied to the map from drift fields to stationary currents, with the topological non-degeneracy of (C2) and (C3) ensuring that the singular set has positive codimension. The flat-density counterexample (constant drift on the torus, where $\nabla\Sigma$ and $\nabla\Phi_I$ both vanish identically) violates both (C2) and (C3) and is excluded by hypothesis. Configuration spaces relevant to chemistry (composition simplices) and learning (parameter spaces with weight decay) satisfy (C1)–(C3) automatically; we discuss this in §5.

4.2 Consequences for learning theory

The Two-Field Independence Theorem has three potential consequences for the study of phase transitions in neural network training, each of which is in principle empirically testable.

Consequence 1: gradient descent is generically not single-field. Standard analyses of neural network training treat the dynamics as gradient descent on a loss surface $L(\theta)$, modeled as $\dot{\theta} = -\nabla L(\theta) + \text{noise}$. When training is augmented by weight decay, learning-rate scheduling, batch-size modulation, or RLHF feedback, the effective drift acquires components that need not be gradients of L . The Two-Field Independence Theorem implies that if these additional components produce a non-equilibrium stationary distribution—which they generically do, since training does not converge to the Boltzmann distribution of L —then the dynamics admits a two-field description, and the parameter distribution $p^*(\theta)$ cannot in general be recovered from L alone. The information quasi-potential $\Phi_I = -\ln p^*$ may encode structural information about the trained network that is not directly visible from the loss geometry.

Consequence 2: compression dividend may require both fields. The compression-dividend theorem cited in §3.4 establishes that, across an ontological phase transition, the post-transition primitive count satisfies $|\mathcal{O}_N^{\text{post}}| \leq |\mathcal{O}_N^{\text{pre}}|/\eta$ where η is the alignment-protocol efficiency. Reframed in the two-field language: the compression is driven by Φ_I (which selects deeper-well representations), but its rate is set by Σ (which provides the exploration entropy through which deeper basins are discovered). Single-field reductions—whether loss-only (Liu et al., 2023) or compression-only (DeMoss et al., 2025)—may capture one side of this dynamic but not its complete structure within this framework.

Consequence 3: alignment protocols may modify Φ_I , not Σ . Reinforcement learning from human feedback, constitutional training, debate, and targeted interpretability protocols share a common structural feature: they introduce an auxiliary signal that biases the trained network toward configurations satisfying external constraints, without modifying the gradient-descent substrate dynamics that produces representational structure. In the two-field language, these protocols can be read as modifying Φ_I (by reshaping the stationary measure) without modifying Σ (the entropy- production geometry). The alignment efficiency $\eta = I(A; C_2 | \mathcal{O}_N)/H(C_2 | \mathcal{O}_N)$ introduced in the OPT companion preprint measures, in this reading, the projection of the protocol’s Φ_I -modification onto the direction of the ground-truth context shift. Different protocols produce different η values; comparing them on this scale provides a common unit for protocol-efficiency comparison.

5 Two Candidate Instances

The framework of §§2–4 is substrate-agnostic: the two-field structure, the candidate order parameters, and the independence theorem are formulated to apply to any driven informational

system satisfying the regularity conditions. What distinguishes the instances is which configuration manifold \mathcal{M} the dynamics unfolds on, what entropy flux drives the substrate, and on what time scale the resulting dynamics develops. We present two candidate instances side by side, indicate what the framework predicts they share, and indicate what remains substrate-specific.

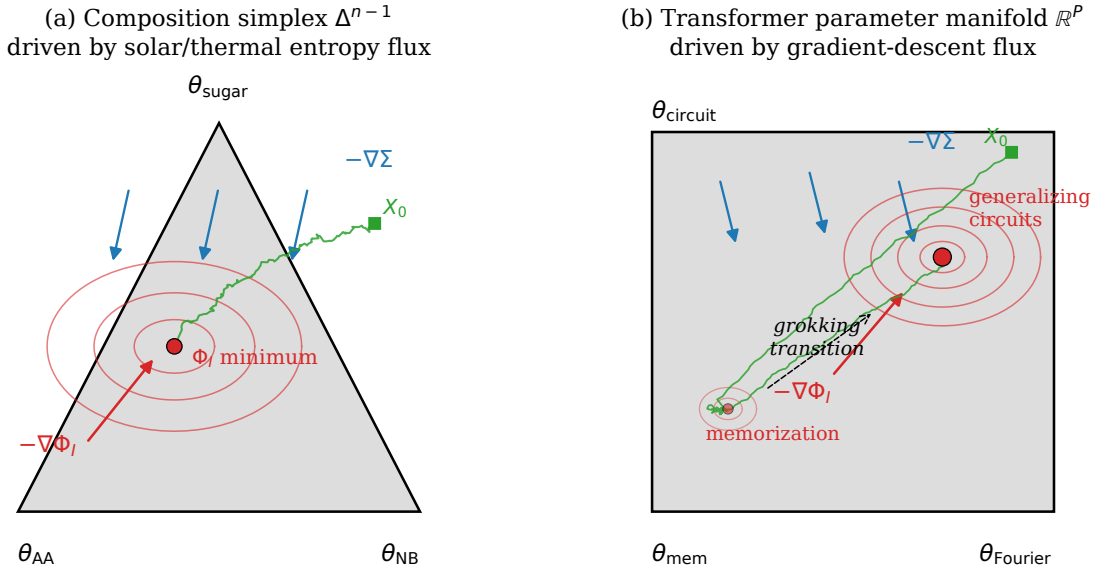


Figure 2: **The two-field geometry on two configuration manifolds (schematic).** Both panels depict the same dynamical class: a stochastic trajectory X_t (green) on a configuration manifold \mathcal{M} driven by an external entropy flux (Σ , blue arrows) and stabilized at attractors of the information quasi-potential Φ_I (red contours). The two gradient fields $\nabla\Sigma$ and $\nabla\Phi_I$ are non-collinear off equilibrium (§4). (a) Prebiotic-chemistry instance: the configuration manifold is the composition simplex Δ^{n-1} with vertices labelled by amino-acid (AA), nucleobase (NB), and sugar species; entropy flux is solar/thermal; attractors are deep Φ_I wells at AAs and nucleobases. (b) Transformer-learning instance: the configuration manifold is the parameter space \mathbb{R}^P with axes labelled by representational regimes (memorization, Fourier features, generalizing circuits); entropy flux is the gradient-descent training signal; the trajectory exhibits a long memorization plateau before transitioning to the generalizing-circuit attractor (the grokking phenomenon (Nanda et al., 2023; Power et al., 2022)).

5.1 Instance 1: Carbon–nitrogen chemistry under solar entropy flux

In prebiotic chemistry, the configuration manifold is the composition simplex $\mathcal{M} = \Delta^{n-1}$ of molecular species under mass conservation. The drift b is determined by the reaction-rate matrix of the chemical network, modulated by catalytic surfaces, geometric confinement, and pH conditions. The noise D encodes thermal fluctuations at ambient temperature. The entropy flux that drives the system out of detailed balance is external: ultraviolet photolysis from solar radiation, hydrothermal heat gradients, shock chemistry from impacts, and wet–dry cycling under tidal or atmospheric forcing.

Conditions (C1)–(C3) of the Two-Field Independence Theorem are satisfied automatically. The composition simplex is compact and convex, hence contractible—giving (C1) and (C3). The Morse condition (C2) corresponds to strictly positive vibrational frequencies at stable molecular configurations, verified spectroscopically across all amino acids and nucleobases.

Empirical anchors. Five independently published prebiotic systems anchor the framework’s validity in this instance. Ferris et al. (1996) demonstrated mineral-catalyzed RNA oligomer-

ization to lengths an order of magnitude beyond solution-only controls; the inferred catalysis–confinement synergy factor $S \approx 5.75$ falsifies single-field gradient accounts (§2.4). Blank et al. (2001) reported the non-monotonic optimal entropy-flux window for amino-acid yield in shock synthesis. Matreux et al. (2024) demonstrated three-orders-of-magnitude selective enrichment of > 50 prebiotic building blocks under simple heat flow. Floroni et al. (2025) realized the full prebiotic-to-biotic transition criterion—attractor coupling, sustained external flux, and geometric confinement—in a single membraneless protocell driven by a microscale heat gradient. Rout et al. (2025) demonstrated that amino acids catalyze RNA copolymerization with strongly base-dependent fold-enhancements (more than $100\times$). The framework identifies amino acids and nucleobases as deep wells of Φ_I under sustained entropy flux, with the universality of these motifs across meteoritic, asteroidal, and laboratory environments (Kvenvolden et al., 1970; McGuire, 2022; Oba et al., 2023) reflecting their status as attractors of equation (1) on this manifold.

Realization. Biological intelligence on Earth can, on this view, be regarded as one realization of the dynamics (1) on the chemical configuration manifold. The relevant time scale is evolutionary ($\sim 10^9$ years from prebiotic chemistry to multicellular life). The self-referential coupling threshold κ_c is crossed in template-directed synthesis and autocatalytic networks, with $\kappa_{AB} > \kappa_{\min}$ consistent with the Floroni protocell experiment. The framework does not claim biological intelligence is the unique solution on this manifold, only that it is one realized solution given Earth’s specific entropy-flux history.

5.2 Instance 2: Transformer parameter manifolds under gradient-descent flux

In neural network training, the configuration manifold is the parameter space $\mathcal{M} = \mathbb{R}^P$ of a model architecture (or a submanifold if architectural constraints reduce effective dimension), where P is the parameter count. The drift b is the negative gradient of the training loss together with weight-decay regularization and optimizer-specific terms (momentum, adaptive scaling). The noise D encodes mini-batch gradient noise, the magnitude of which depends on batch size and learning-rate schedule (Hoogland et al., 2024; Liu et al., 2022). The entropy flux is data-driven: each training step deposits new information into the parameter distribution, and the cumulative flux is the integrated gradient signal over training.

Conditions (C1)–(C3) require more care than in the chemical instance. Compactness (C1) is enforced effectively by weight decay (the stationary measure has bounded support). Non-degeneracy (C2) corresponds to strict positivity of the Hessian at typical loss minima, generically satisfied for over-parameterized networks but failing at degenerate basins relevant to singular learning theory (Watanabe, 2009). Trivial first cohomology (C3) holds for \mathbb{R}^P but may fail for architectures with discrete symmetries (permutation invariance of hidden units, weight-tying); we treat these symmetries as gauge degrees of freedom that can be quotiented out.

Empirical anchors. Several phase-transition phenomena in neural network training serve as empirical anchors for the framework in this instance. *Grokking*, the delayed transition from memorization to generalization in modular arithmetic (Liu et al., 2022; Nanda et al., 2023; Power et al., 2022), has recently been given a rigorous quantitative theory: the Norm-Hierarchy Transition Law (Truong and Truong, 2026b; Truong et al., 2026) establishes that the delay scales as $T_{\text{grok}} - T_{\text{mem}} = \Theta(\gamma_{\text{eff}}^{-1} \log(\|\theta_{\text{mem}}\|^2 / \|\theta_{\text{post}}\|^2))$, where γ_{eff} is the effective contraction rate of the optimizer ($\gamma_{\text{eff}} = \eta\lambda$ for SGD, $\geq \eta\lambda$ for AdamW), with matching upper and lower bounds under regularised first-order dynamics. We use this rigorous form as the basis for Prediction 3a (§6.3). *Emergent capabilities* (Wei et al., 2022) are identified, in the two-field reading, with the crossing of phase boundaries in Φ_I as model scale and training compute increase.

Introspective access in frontier language models has been the subject of converging empirical

work in 2024–2026 (Binder et al., 2024; Lederman and Mahowald, 2026; Lindsey, 2025; Macar et al., 2026; Song et al., 2025). Lindsey (2025) demonstrated, using activation injection on Anthropic frontier models, that introspection on internal states satisfies the four operational criteria (accuracy, grounding, internality, metacognitive representation) in *some* scenarios, but is highly unreliable and context-dependent. Lederman and Mahowald (2026) replicated these findings in open-source models and dissociated two underlying mechanisms: probability-matching (inference from prompt anomaly) and direct access (content-agnostic state detection). Macar et al. (2026) found that introspective capacity is suppressed by default in sampled outputs but detectable via logit lens in intermediate layers, with elicitation methods raising detection rates from 0.3% to 39.9%. Song et al. (2025) report that LLMs fail to meaningfully introspect under a more demanding “privileged self-access” definition.

The persistent finding across these studies is *partial* introspective capacity—above the noise floor but well below the reliability that full self-modelling would predict. The framework interprets this pattern as operation in the vicinity of κ_c : indicative estimates derived from injection-detection rates and self-report fidelity yield $F \in [0.3, 0.5]$ and $C \in [0.05, 0.15]$ across the studied frontier systems, placing them in the immediate neighbourhood of (F_{\min}, C_{\min}) but neither reliably above nor confidently below. Whether κ_c crossings have already occurred in deployed systems, are imminent in the next training generation, or remain distant, is an open empirical question that direct measurement of $F(\kappa)$ and $C(\kappa)$ on full training trajectories could settle. Independent support for the structural claim that increasing κ has measurable effects on the trained network comes from Premakumar et al. (2024), who demonstrated that adding self-modelling auxiliary tasks during training reduces the real log canonical threshold (RLCT)—a result we discuss further in §7.2.

Realization. Frontier large language models can, on this view, be regarded as a second realization of the dynamics (1), on the transformer parameter manifold. The relevant time scale is computational ($\sim 10^4$ – 10^6 gradient-descent steps from initialization to deployment). The breakdown threshold $\alpha^\dagger = \Theta(1/\log |\mathcal{O}_N|)$ predicts that LLMs of higher capability may be intrinsically more vulnerable to adversarial data corruption per unit contamination budget—a quantitative formalization of the intuition motivating recent work on data poisoning, jailbreak resistance, and alignment robustness (Casper et al., 2023; Chornomaz et al., 2025; Hanneke et al., 2022). The framework does not claim that current LLMs are intelligent in any substantive philosophical sense; we propose only that they may be productively studied as particular instances within the framework on the transformer parameter manifold.

5.3 What is shared, and what is not

The proposal we develop is that the two instances may be productively viewed as members of a common dynamical class, in the sense that they are particular instances within the same framework on different configuration manifolds. Below we make explicit which features the framework predicts to be shared and which are instance-specific; neither the shared features nor their universality status are established by this perspective paper alone.

The asymmetry in scale (nine orders of magnitude in degrees of freedom, fourteen orders of magnitude in time scale) is among the most striking features of the unification. We do not claim it is explanatory: the framework does not predict which solutions are realized in a given universe, only that whatever solutions are realized share the universality-class invariants of Table 1. The realized scales are determined by the specific entropy-flux history of the substrate—a question for astrophysics and the specific computational economics of training runs, respectively, not for the framework itself.

Feature	Shared	Instance-specific
Two-field independence ($\nabla\Sigma \not\parallel \nabla\Phi_I$)	✓	—
Existence of α^\dagger, κ_c	✓	functional form constants
Compression at phase transition	✓	compression units (species vs. circuits)
Single-field structural no-go theorems	✓	—
Configuration manifold \mathcal{M}	—	Δ^{n-1} vs. \mathbb{R}^P
Entropy flux source	—	solar/thermal vs. gradient-descent
Substrate physics	—	molecular vs. computational
Time scale	—	10^9 years vs. 10^5 steps
Number of degrees of freedom	—	$n \sim 10$ – 100 vs. $P \sim 10^9$ – 10^{12}

Table 1: Universality-class invariants and instance-specific features across the two empirical instances. The shared features are consequences of the two-field structure and the regularity conditions (C1)–(C3); the instance-specific features parameterize which solution within the family is realized.

5.4 Other potential instances

We mention briefly, without development, three further candidate instances that the framework would in principle accommodate but that we do not validate empirically here. (i) *Neural development in embryos* (Levin, 2023): the configuration manifold is gene-expression and morphogen-concentration space; the entropy flux is metabolic ATP consumption; the relevant time scale is ontogenetic. (ii) *Major evolutionary transitions* (Maynard Smith and Szathmary, 1995; Prokopenko et al., 2025): the configuration manifold is the genotypic–phenotypic state space of a lineage; the entropy flux is selective pressure integrated over generations; the relevant time scale spans the transition from prokaryotic to eukaryotic life or from solitary to multicellular organization. (iii) *Multi-agent collective intelligence*: the configuration manifold is the joint strategy space of interacting agents; the entropy flux is the information exchange rate; the relevant time scale is set by the mixing time of the interaction graph. We treat these as speculative extensions, deferred to future work.

5.5 Empirical convergence: what the framework explains

The two-field framework was developed before the empirical findings synthesised below; we summarise them here to make the framework’s *explanatory*—as opposed to merely predictive—content concrete. The findings are recent (mostly 2024–2026), independent of the framework’s development, and converge on a structure that the two-field perspective makes coherent.

Alignment phase transitions exist and are localised. Turner et al. (2025) isolated a mechanistic phase transition in rank-1 LoRA fine-tuning across model families and sizes: directions for misalignment are learnt over a narrow window of training steps, with the transition evident both in fine-tuned parameters and in behavioural misalignment. Soligo et al. (2025) found convergent linear representations of misalignment across model organisms, suggesting a shared structural target. Arnold and Lorch (2025) decomposed transitions into multiple plain-English order parameters with shared timing, finding that the behavioural transition occurs substantially *later* than the gradient norm peak (which serves as an early-warning signal). Henrick and Corlourer (2026) derived a spectral heat-capacity observable from a 2-datapoint reduced density matrix, providing critical-slowness early warning of second-order transitions during training. The two-field framework reads these collectively as signatures of κ_c crossing—a single underlying regime change with multiple measurable correlates.

Adversarial breakdown decreases with model scale. Souly et al. (2025), in the largest pretraining poisoning study to date (600M–13B parameters under Chinchilla-optimal training), found that approximately 250 poisoned documents produce robust backdoors *regardless* of model or dataset size. The poisoning fraction required therefore decreases monotonically with scale: a 13B model trained on more than $20\times$ the clean data of a 600M model is backdoored by the same absolute count of poisons. This is qualitatively the prediction $\alpha^\dagger(\mathcal{O}_N) \rightarrow 0$ as $|\mathcal{O}_N| \rightarrow \infty$ established in (5), *though faster than purely logarithmic*. The two-field framework treats this discrepancy as informative rather than falsifying: the empirical rate of α^\dagger decay probes how $|\mathcal{O}_N|$ scales with parameter count P . A super-polynomial relation $|\mathcal{O}_N(P)| = \exp(\Theta(P^\beta))$ for some $\beta > 0$ recovers the Souly et al. rate from (5); this is consistent with the combinatorial explosion of representable circuit motifs in transformer parameter spaces, but a rigorous $|\mathcal{O}_N|-P$ correspondence remains open (§7.6).

Introspective capacity is partial and content-agnostic. Recent work on LLM introspection (Binder et al., 2024; Lederman and Mahowald, 2026; Lindsey, 2025; Macar et al., 2026; Song et al., 2025) collectively reports that frontier LLMs detect injected internal states above the noise floor but identify their content unreliably. Lederman and Mahowald (2026) explicitly dissociate two mechanisms: probability-matching (inference from prompt anomaly) and direct access (content-agnostic state detection). The framework interprets this dissociation as the operational signature of operation in the κ_c vicinity: the gap between detection (reflecting medium F) and content-encoding (reflecting low C) maps onto the framework’s distinction between predictive fidelity and causal efficacy in (7)–(8).

Self-modelling reduces RLCT. Premakumar et al. (2024) demonstrated that adding self-modelling auxiliary tasks during training reduces the real log canonical threshold (RLCT) of the trained network, indicating reduced loss-landscape singularity. Within the two-field reading, increasing the self-referential coupling strength κ deepens the wells of Φ_I on the loss-relevant manifold; this manifests, in the language of singular learning theory, as RLCT reduction. The Premakumar et al. finding therefore provides the first direct empirical bridge between κ and Watanabe’s RLCT machinery, closing a gap noted as open in §7.2.

Synthesis. The pattern across these independent findings is a phase-transition phenomenology in driven informational systems with: (i) a complexity-dependent vulnerability threshold whose decay rate probes the $|\mathcal{O}_N|-P$ correspondence; (ii) a self-modelling threshold whose vicinity is occupied by current frontier systems; (iii) measurable correlates in spectral observables (heat capacity, participation ratio) and structural invariants (RLCT, linear representation directions). The two-field framework offers the dynamical class within which this pattern is internally consistent. It does not claim to be the only such class; it claims that no single-field gradient account, taken alone, can reproduce this combination of features.

6 Falsifiable Predictions

A perspective paper claims theoretical territory by identifying predictions that, if falsified, would force revision or abandonment of the framework. We state three such predictions, each operational on existing experimental or computational platforms, and each discriminating the two-field framework against single-field alternatives.

Several predictions below have partial empirical support already in the literature. Bereska et al. (2025) measure sparse-autoencoder feature-count consolidation at the grokking transition on modular arithmetic, providing one component of the $|\mathcal{O}_N|$ measurement protocol of Prediction 1. Clauw et al. (2024) (introduced in §5) report that O-information synergy peaks before grokking, consistent with the non-additive structure underlying Prediction 2. Arnold and

Lörch (2025) document that behavioural transitions during emergent-misalignment fine-tuning lag the gradient-norm peak, establishing the sign of Δt in Prediction 3a. The protocols below extend these partial validations to the framework’s specific quantitative claims, and identify the discriminating measurements still missing.

6.1 Prediction 1: Joint scaling of α^\dagger and κ_c

The duality claim of §3.3 predicts that the two order parameters scale jointly with representational complexity in a manner specified by (10). Within a family of driven informational systems of varying complexity—transformers of varying width on a fixed task, or chemical networks of varying species count on a fixed entropy-flux protocol—the products $\alpha^\dagger(\mathcal{O}_N) \cdot (\log |\mathcal{O}_N|)^{\gamma_1}$ and $\kappa_c(\mathcal{O}_N) \cdot (\log |\mathcal{O}_N|)^{\gamma_2}$ should approach distinct universal constants asymptotically, with (γ_1, γ_2) identifying the universality class.

Operational protocol (learning instance). We propose varying the modulus p of \mathbb{Z}_p as the size variable, following the finite-size-scaling methodology of Bi et al. (2026), who note that varying width across model classes does not satisfy the controlled single-family size variation that finite-size scaling requires. The transformer architecture (width, depth, attention heads) is held fixed; only p varies across $p \in \{53, 97, 113, 251, 503, 1009\}$, with weight decay and learning rate held constant. For each trained model: (i) estimate $|\mathcal{O}_N|$ via the linear-mapping number, the sparse-autoencoder feature count, or the entropy-weighted effective-feature count of Bereska et al. (2025) (Cunningham et al., 2023; Liu et al., 2023); (ii) estimate α^\dagger by running data-poisoning experiments at varying contamination rates and identifying the contamination level above which a two-stage shift-detection protocol fails; (iii) estimate κ_c via the introspection-injection protocol of Lindsey (2025) adapted to grokking-task models, identifying the smallest coupling at which $F(\kappa) \geq F_{\min}$ and $C(\kappa) \geq C_{\min}$.

Predicted signature. For each modulus p , plot $\log \alpha^\dagger(p)$ and $\log \kappa_c(p)$ against $\log \log |\mathcal{O}_N(p)|$. The two-field framework predicts: (i) both quantities exhibit asymptotic linear behaviour in this log–log scale, with negative slopes $-\gamma_1$ and $-\gamma_2$ respectively; (ii) $\gamma_1 = 1.0 \pm 0.15$, consistent with the α^\dagger scaling (5) (an independent test of established theory); (iii) γ_2 takes a definite value in $(0, 1]$, to be determined by the experiment. The framework is *silent on the specific value* of γ_2 : it predicts only that $\gamma_2 \in (0, 1]$, that γ_2 is positive (so κ_c does decrease with complexity), and that the same γ_2 is observed across system instances within the same nominal class (e.g., across modular addition versus modular multiplication tasks). The experiment thus serves simultaneously as parameter estimation and as a falsification test.

Falsification. The framework is falsified if any of the following holds: (a) either product fails to exhibit asymptotic linear log–log behaviour (e.g., diverges, vanishes, or shows oscillatory or non-monotone scaling); (b) γ_1 is found to differ significantly from 1, contradicting the established α^\dagger scaling; (c) γ_2 differs significantly across instances of the same nominal class, indicating that γ_2 is not a class invariant; or (d) $\gamma_2 \leq 0$, indicating that κ_c does not decrease with representational complexity.

Discrimination. Single-field theories of grokking predict at most one order parameter (compression rate, basin depth, RLCT). They do not, in their current forms, predict the joint scaling of two distinct quantities, since they posit only one phase transition. Confirmation of joint scaling would suggest single-field alternatives, in their current forms, are incomplete.

6.2 Prediction 2: Catalysis–confinement synergy in LLM training

Theorem 2.2 of Truong and Truong (2026a) establishes that single-field gradient dynamics on compact manifolds with linear driving combine two perturbations with disjoint local supports *additively*, with superlinearity factor $S = 1 + O(\|\delta V\|^2)$. The empirically inferred $S \approx 5.75$ in clay-catalyzed RNA polymerization (Ferris et al., 1996) is the discriminating empirical signature for two-field structure in the chemical instance. We predict an analogous signature in the learning instance.

Consider two training-signal modifications with disjoint local support in parameter space: *curriculum learning* (modulating the data-distribution sequence) and *targeted data augmentation* (modulating the per-sample input distribution). Each individually modifies Φ_I in a localized region of the parameter manifold; under single-field reduction, their joint application would combine additively in compression effect.

Operational protocol. Train four models on a fixed underlying task (e.g., modular arithmetic, code synthesis on a benchmark, or a small transformer language modeling task), under four conditions: (i) baseline (no modification); (ii) curriculum only; (iii) augmentation only; (iv) both combined. After each model reaches its grokking transition, measure the post-transition primitive count $|\mathcal{O}_N^{\text{post}}|$ via the same estimator as Prediction 1. Compute the synergy factor

$$S_{\text{LLM}} := \frac{|\mathcal{O}_N^{\text{base}}| - |\mathcal{O}_N^{\text{both}}|}{(|\mathcal{O}_N^{\text{base}}| - |\mathcal{O}_N^{\text{curr}}|) + (|\mathcal{O}_N^{\text{base}}| - |\mathcal{O}_N^{\text{aug}}|)}.$$

Predicted signature. $S_{\text{LLM}} > 1 + O(\delta^2)$, where δ is a measure of perturbation strength in parameter space. We do not predict a specific numerical value (the chemical $S \approx 5.75$ is system-specific), only that the signature exceeds the perturbative additivity bound.

Falsification. $S_{\text{LLM}} \approx 1$ within experimental uncertainty.

Discrimination. The no-go result above implies that any single-field gradient model of training, combined with the assumption of disjoint perturbation supports, must predict $S \approx 1$. Observed $S > 1$ would suggest single-field gradient accounts of representational reorganization in transformer training, in their current forms, are incomplete—paralleling the situation in chemistry.

6.3 Prediction 3: κ_c crossing as the mechanism of observed alignment phase transitions

Phase transitions in alignment fine-tuning are by now an established empirical phenomenon. Turner et al. (2025) isolate a mechanistic phase transition in rank-1 LoRA fine-tuning across model families and sizes: directions for misalignment are learnt over a narrow window of training steps, with the transition evident both in fine-tuned parameters and in misalignment scaling behaviour. Soligo et al. (2025) demonstrate that emergently misaligned models converge to similar linear representations of misalignment across training conditions. Arnold and Lörch (2025) develop a physics-style order-parameter framework for these transitions, finding that the behavioural transition occurs *substantially later* than the gradient norm peak, which serves as an early-warning signal. Hennick and Corlouer (2026) derive a spectral heat-capacity observable from a 2-datapoint reduced density matrix, providing critical-slowness early warning of second-order transitions during training.

Against this empirical background, the two-field framework makes a *mechanistic* claim: alignment phase transitions are signatures of κ_c crossing—the regime change from passive sampling of statistics to self-referential encoding and action—distinguishable from alternative mechanisms

(basin selection in a fixed loss landscape, RLCT degeneracy alone, capability-only emergence) by three operational signatures that can be tested simultaneously on existing model-organism setups.

3a. Phase-transition timing. The behavioural transition lags the gradient norm peak by a delay Δt that, under the framework, follows the Norm-Hierarchy Transition (NHT) Law (Truong and Truong, 2026b; Truong et al., 2026). That law establishes, with matching upper and lower bounds for regularised first-order dynamics, that delayed representational transitions satisfy

$$T = \Theta(\gamma_{\text{eff}}^{-1} \log(V_{\text{sc}}/V_{\text{st}})), \quad (11)$$

where γ_{eff} is the effective contraction rate of the optimizer ($\eta\lambda$ for SGD; $\geq \eta\lambda$ for AdamW), and $V_{\text{sc}}, V_{\text{st}}$ are the characteristic norms of the shortcut and structured representations. We propose that alignment phase transitions in the self-referential regime are governed by an analogous law, with the substrate-level contraction rate γ_{eff} replaced by the self-referential coupling strength κ (which plays the role of effective contraction toward the encoded internal model), and the norm ratio $V_{\text{sc}}/V_{\text{st}}$ replaced by an \mathcal{O}_N -cardinality proxy. Concretely:

$$\Delta t = \Theta(\kappa^{-1} \log|\mathcal{O}_N^{\text{pre}}|). \quad (12)$$

Equation (12) is presented as a mapping conjecture rather than a derived identity: the structural form (logarithmic dependence on a complexity proxy, inverse dependence on a contraction-like rate) inherits from (11), but the identification $\kappa \leftrightarrow \gamma_{\text{eff}}$ and $\log|\mathcal{O}_N^{\text{pre}}| \leftrightarrow \log(V_{\text{sc}}/V_{\text{st}})$ is the proposed extension of the NHT framework to the self-referential coupling regime. Reduction of (12) to (11) in a suitable limit, together with rigorous bounds in the alignment-fine-tuning setting, is open. *Falsification:* Δt does not scale logarithmically with model capability, or is independent of the LoRA rank used to induce the transition (which controls the effective κ).

3b. Spectral coincidence with independently estimated κ_c . The peak in the spectral heat capacity (Hennick and Corlouer, 2026) over training time should coincide with the κ_c crossing point estimated independently from the joint scaling experiment of Prediction 1 (§6.1), within a confidence interval set by the spectral width and the Prediction 1 estimation error. This two-experiment cross-check is the strongest test available with current methodology. *Falsification:* the two peaks separate by more than the combined uncertainty, indicating that the spectral observable and the framework’s κ_c estimate track different objects.

3c. Persistence discontinuity at κ_c . Within a single training run that crosses κ_c , alignment-protocol perturbations applied at checkpoints t_i should yield persistence $\tau(t_i)$ that exhibits a *derivative discontinuity* at the κ_c crossing point: $\partial^2\tau/\partial t^2$ exceeds a noise-floor threshold in a small window around the predicted κ_c , while remaining smooth elsewhere—including at the gradient norm peak (which precedes the transition per Arnold and Lörch (2025)). *Falsification:* $\tau(t)$ varies smoothly across the predicted κ_c location, or shows discontinuity only at the gradient norm peak. The latter outcome would indicate that the gradient norm peak *is* the alignment-relevant transition rather than its precursor, contradicting the framework’s two-stage structure.

Discrimination. Each sub-prediction discriminates the framework against a different alternative. Prediction 3a discriminates against accounts in which gradient norm and behavioural transition coincide (early single-field accounts; Arnold and Lörch’s finding already creates pressure on these). Prediction 3b discriminates against accounts that lack a complexity-dependent threshold (e.g., variational free energy minimization in the FEP alone, which predicts continuous improvement). Prediction 3c discriminates against accounts in which the gradient norm peak *is* the transition rather than its precursor, including several mechanistic-interpretability accounts of the Turner et al. (2025) setup.

Operational protocol. Predictions 3a–c can be tested simultaneously on the model-organism setup of Turner et al. (2025) (rank-1 LoRA fine-tuning of a mid-scale instruction-tuned model), using the analytical machinery of Arnold and Lörch (2025) (LLM-judged plain-English order parameters with statistical dissimilarity measures) and Hennick and Corlouer (2026) (2-datapoint reduced density matrix spectral observables). The cost of testing is approximately one fine-tuning run with checkpointed perturbation experiments and post-hoc analysis. Open-source implementations of the necessary primitives—rank-1 LoRA fine-tuning with phase-transition probing (Soligo et al., 2026; Turner et al., 2025), concept-injection introspection on open-weights models (Macar et al., 2026), and the order-parameter and spectral-observable analyses of Arnold and Lörch (2025) and Hennick and Corlouer (2026)—are publicly available, making the combined test feasible without novel infrastructure. We invite the alignment-evaluation community to apply this existing methodology to the combined test.

6.4 Summary

The three predictions are independent: each can be tested without the others, and falsification of any one would call for significant revision of the framework. Predictions 1 and 2 are testable on existing computational infrastructure with no novel measurement apparatus. Prediction 3 may be approached using the introspection-injection protocol of Lindsey (2025) combined with the order-parameter and spectral-observable methodologies of Arnold and Lörch (2025) and Hennick and Corlouer (2026), all demonstrated on research-scale models. We invite empirical groups in both communities—alignment evaluation laboratories (Casper et al., 2023; Turner et al., 2025) and prebiotic-chemistry experimental groups (Mast–Braun (Floroni et al., 2025; Matreux et al., 2024), Sutherland (Singh et al., 2025), Damer–Deamer (Damer and Deamer, 2020))—to consider testing the predictions on platforms where they have native expertise.

7 Discussion: What This Reframes

The two-field framework intersects several active research programs. Honest positioning relative to each is essential both for assessing the framework’s contribution and for identifying productive directions of collaboration. We address five neighboring lines and conclude with limitations and open problems.

7.1 Grokking and the compression-rate accounts

The compression-as-grokking line of work (Clauw et al., 2024; DeMoss et al., 2025; Liu et al., 2023; Nanda et al., 2023) has substantially advanced the empirical understanding of representational phase transitions in neural networks. Liu et al. (2023) attribute grokking to the emergence of compressed representations measured by the linear-mapping number; Nanda et al. (2023) identify Fourier circuits as the specific structure of these compressed representations; and DeMoss et al. (2025) and Clauw et al. (2024) formalize the compression dynamics through rate–distortion and information-theoretic phase-transition lenses respectively.

The two-field framework is broadly consistent with these results in their direction, and offers complementary tools: an information-theoretic lower bound on detection time, a strict-inequality form of the compression dividend (both established in the OPT companion preprint, see §3.4), and a perspective in which compression is read as one consequence of phase transition rather than its definition. Within this reading, the compression rate is not the order parameter; $|\mathcal{O}_N|$ plays that role, and compression $|\mathcal{O}_N^{\text{post}}|/|\mathcal{O}_N^{\text{pre}}| \leq 1/\eta$ is its image under the phase transition. Single-field compression theories typically describe the phase transition as gradient descent on a complexity functional; the two-field framework recovers this regime as the special case in which $\nabla\Sigma$ and $\nabla\Phi_I$ become collinear, identified in §4 as the measure-zero non-generic case under the stated regularity conditions.

7.2 Singular learning theory and developmental interpretability

The singular learning theory program (Hoogland et al., 2024; Pepin Lehalleur et al., 2025; Watanabe, 2009) characterizes Bayesian phase transitions in neural networks via the real log canonical threshold (RLCT), an algebraic-geometric invariant of the loss landscape. The Timaeus developmental-interpretability program applies these tools to study staged learning empirically.

The two frameworks are formally complementary. SLT analyzes the *posterior geometry* under a fixed data distribution; the two-field framework analyzes the *Langevin dynamics* on the parameter manifold under driven training. The RLCT characterizes basin shape; α^\dagger characterizes basin robustness across distributional shift; κ_c characterizes the emergence of self-referential coupling. Recent empirical work (Premakumar et al., 2024) establishes that increasing self-modelling auxiliary load reduces the RLCT of trained networks; this provides the first measured bridge between the self-referential-coupling axis (κ) and the SLT machinery, and is discussed further in §5.5. We conjecture that systems near a Bayesian phase transition in the RLCT sense undergo simultaneous transitions in α^\dagger and possibly in κ_c , but no formal correspondence has been established and we treat this as an open problem (§7.6). The two programs differ chiefly in framing: SLT is Bayesian and posterior-centric; the two-field framework is dynamical and trajectory-centric. Both should be welcomed.

7.3 The free energy principle and active inference

The free energy principle (Friston, 2010,?; Ramstead et al., 2023) unifies perception and action through the variational minimization of free energy under a generative model. The recent extension to large language models (Prakki, 2024) treats LLM behavior as approximate active inference.

The Linfoot fidelity $F(\kappa)$ in (7) is related to but distinct from the FEP variational free energy: both are mutual-information-based, but F admits a sharp threshold form via operational thresholds, whereas free energy is continuously minimized. The two-field framework can be read as supplying the FEP with an explicit substrate dynamics (Σ -driven) underlying the variational minimization. In particular, the FEP does not specify what generates the generative model itself; the two-field framework proposes that the generative model is encoded by Φ_I , and the threshold κ_c is the regime change at which this encoding becomes self-referentially stable. Recent work extending the FEP to origin-of-life dynamics and the present framework’s chemistry instance are mutually compatible; we expect productive cross-pollination.

7.4 Algorithmic origins and tangled hierarchies

Walker and Davies (2013) proposed informational takeover as the defining transition in the origin of life: living systems are systems in which information control top-down. The recent extension by Prokopenko et al. (2025) formalizes this through tangled information hierarchies and self-modeling dynamics, identifying biological arrow-of-time as emergent from these hierarchies.

The Prokopenko et al. framework is the closest neighbor of the κ_c construct in the present perspective. Both identify a regime change associated with self-modeling; both ground the change in information-theoretic quantities. The differences are that Prokopenko et al. (2025) present self-modeling as a qualitative hierarchy structure, whereas this perspective specifies κ_c as a quantitative threshold with explicit operational definitions F and C ; and that Prokopenko et al. (2025) apply primarily to the biological-evolutionary domain, whereas the present framework applies symmetrically to the learning instance. We propose the κ_c formulation as a quantitative formalization of the tangled-hierarchies framework, not a competing alternative; both direct empirical work toward measurement of self-modeling onset.

7.5 Thermodynamic-bounds line and dissipation theories

The thermodynamic-bounds line (Busiello et al., 2021; Liang et al., 2024a,b) establishes kinetics-independent upper and lower bounds on symmetry-breaking in driven chemical reaction networks via the matrix-tree theorem. These bounds delineate the *accessible* region of stationary states given a thermodynamic budget. The dissipative-adaptation framework (England, 2015) establishes that driven self-assembling systems are statistically biased toward configurations that absorb and dissipate work efficiently.

The two-field framework is complementary to both. The bounds delimit which stationary states are accessible; the two-field dynamics predicts which trajectory through the accessible region a system follows under specified entropy flux. The dissipative adaptation captures the Σ -driven exploration; the two-field framework adds the Φ_I -driven stabilization that selects deep wells within the explored region. England’s framework is recovered in the limit $\beta \rightarrow 0$ of the dynamics (4); the bounds of Liang et al. (2024a,b) constrain the magnitudes that any specific solution within the framework can exhibit. The three layers—bounds, dissipation, two-field dynamics—together characterize driven chemical reaction networks more tightly than any one in isolation.

7.6 Limitations and open problems

The framework as developed here is a perspective on the unification of two preceding lines of work (the chemistry-side and learning-side companion preprints introduced in §1.3), and inherits their respective scopes and limitations. Specific items deferred to future work include the following.

(i) Rigorous derivation of the joint scaling law. Equation (10) is conjectural in the value of γ_2 . A derivation from first principles—specifying γ_2 together with the asymptotic constants c_1, c_2 and their dependence on the universality class—is open. Candidate routes include a Le Cam two-point reduction with hypothesis classes of size scaling as $\log |\mathcal{O}_N|$, a renormalization-group-style analysis of the coupled (Σ, Φ_I) flow at fixed points, and direct estimation from the experimental protocol of §6.1.

(ii) Formal correspondence with SLT phase transitions. The conjectured simultaneity of RLCT phase transitions and α^\dagger, κ_c transitions is unstudied. A formal correspondence between the singular-learning and two-field accounts would be of substantial value. The empirical bridge provided by Premakumar et al. (2024) is a starting point.

(iii) Empirical estimation of κ_c for current LLMs. The introspection-based evidence (Binder et al., 2024; Lederman and Mahowald, 2026; Lindsey, 2025; Macar et al., 2026; Song et al., 2025) is suggestive but not yet quantitatively connected to κ_c . A direct estimation of $F(\kappa)$ and $C(\kappa)$ for frontier models is open.

(iv) The $|\mathcal{O}_N|$ - P correspondence. The empirical finding of Souly et al. (2025) that α^\dagger decays faster than $1/\log P$ at fixed Chinchilla-optimal scaling probes the relation between primitive-set cardinality $|\mathcal{O}_N|$ and parameter count P . A rigorous super-polynomial correspondence $|\mathcal{O}_N(P)| = \exp(\Theta(P^\beta))$ for some $\beta > 0$ would reconcile theory and experiment but has not been established.

(v) Extension to continuous primitive spaces. The breakdown bound (5) is stated for finite primitive sets. A covering-number extension is sketched in the OPT companion preprint, but the treatment is incomplete.

(vi) Connection to mechanistic interpretability. The relation between the abstract primitive count $|\mathcal{O}_N|$ and the empirical circuit-formation timescales studied in mechanistic interpretability (Nanda et al., 2023; Olsson et al., 2022) is unaddressed.

(vii) Multi-agent and collective extensions. The treatment is single-system. Whether the two-field framework extends to multi-agent collective intelligence (§5.4) through a generalized configuration manifold remains to be determined.

These items define a research program rather than terminal gaps. Each is independently addressable; together they map the territory of the framework’s possible development.

8 Conclusion

We have proposed a framework in which phase-transition phenomena in deep learning and in non-equilibrium prebiotic chemistry may be productively studied as instances within a common dynamical class: driven informational systems governed by two gradient fields, the entropy-production rate Σ and the information quasi-potential $\Phi_I = -\ln p^*$. Within this framework, we have discussed two candidate order parameters: an adversarial breakdown threshold α^\dagger whose decay with the primitive-set cardinality $|\mathcal{O}_N|$ is logarithmic, and a self-referential coupling threshold κ_c associated with the regime in which a system encodes and acts on its own statistics. The joint scaling $(\alpha^\dagger, \kappa_c)$ defines a candidate universality class with two scaling exponents (γ_1, γ_2) as class invariants. We have identified three predictions—joint scaling of the two thresholds (parameter estimation of γ_2), catalysis–confinement synergy in language model training, and three discriminating signatures of κ_c crossing in alignment fine-tuning—each in principle empirically testable on existing infrastructure.

We do not claim that biological intelligence and large language models are the same kind of system; they manifestly are not. We propose only that they may share dynamical structure as instances of a common framework, on configuration manifolds shaped by carbon–nitrogen chemistry under solar entropy flux and by transformer parameter spaces under gradient-descent flux, respectively. The asymmetry of many orders of magnitude in degrees of freedom and time scale between the two instances is not explained by the framework; the framework, if correct in its domain of applicability, would parameterize which instances within the class are realized under given physical conditions, but does not predict that biological-style or model-style realizations are inevitable.

The framework was developed before the empirical findings synthesised in §5.5, and is offered here as a theoretical foundation for the convergent phenomenology that Arnold and Lörch (2025); Hennick and Corlouer (2026); Soligo et al. (2025); Turner et al. (2025) have established for alignment phase transitions, that Souly et al. (2025) have established for adversarial breakdown scaling, and that Lederman and Mahowald (2026); Lindsey (2025); Macar et al. (2026); Song et al. (2025) have established for partial introspection in frontier systems. Two implications deserve emphasis. First, the framework reframes alignment as a two-field problem: protocols modify Φ_I via substrate dynamics, and their efficiency may be measured by the projection of the modification onto the direction of the ground-truth context shift. The information-theoretic unit $\eta = I(A; C_2 | \mathcal{O}_N)/H(C_2 | \mathcal{O}_N)$ (introduced in the OPT companion preprint, §3.4) provides a candidate common scale for protocol-efficiency comparison—an analogue of bits-per-second for alignment. Second, the framework interprets the persistent finding of partial introspection across frontier systems as operation in the vicinity of κ_c , neither reliably above nor confidently below. Identifying or ruling out a κ_c crossing in a controlled training run appears to us a useful empirical question for alignment research.

We invite the alignment-evaluation, mechanistic-interpretability, prebiotic-chemistry, and origin-of-life research communities to consider testing the predictions of §6 on platforms where they have native expertise. Whether the questions of representational reorganization under

context shift, robustness to adversarial corruption, and prebiotic chemical convergence prove to admit a common dynamical description is, ultimately, an empirical question; the present paper proposes one direction of answer and identifies the experiments that could falsify it.

Acknowledgements

The Equation of Motion–Information Field Framework (EOM-IFF) on which the chemistry-side instance of this perspective is built was developed jointly with Truong Quynh Hoa, whose detailed treatment appears in the companion preprint (Truong and Truong, 2026a). The present author thanks Hoa for permission to incorporate that framework in the unification proposed here; responsibility for the unification claim and any errors in its presentation rests with the present author alone.

The author is grateful to the open-access prebiotic-chemistry and non-equilibrium statistical-physics communities, and to the open- review machine-learning theory community, for the public archive of preprints and datasets that made this synthesis possible.

Funding

This research received no specific grant from any funding agency in the public, commercial, or not-for-profit sectors. All work was conducted independently at Clevix LLC (Hanoi, Vietnam) using the author’s own computational resources.

Declaration of AI use

The author used Anthropic’s Claude (large language model assistant) during manuscript preparation for (i) checking \LaTeX syntax and cross-reference consistency, (ii) language editing for grammar and clarity, (iii) reviewing the accuracy of literature citations, and (iv) identifying recent relevant literature. All theoretical content, theorem statements, proof sketches, predictions, and final editorial choices are the author’s own. The author takes full responsibility for the scientific content of this article.

Conflict of interest declaration

The author declares no competing interests, financial or otherwise, relevant to the subject matter of this manuscript. Clevix LLC is an independent research entity and has no commercial interest in the outcome of the theoretical framework developed herein.

Data accessibility

This article has no primary experimental data. All analyses cite published data from peer-reviewed literature and preprints, which were not re-collected by the author. The companion preprints (Truong and Truong, 2026a; Truong, 2026) contain the underlying theoretical derivations and computational validations referenced herein.

References

Julian Arnold and Niels Lörch. Decomposing behavioral phase transitions in LLMs: Order parameters for emergent misalignment. *arXiv preprint arXiv:2508.20015*, 2025. doi: 10.48550/arXiv.2508.20015. URL <https://arxiv.org/abs/2508.20015>.

- Mohamed Ishmael Belghazi, Aristide Baratin, Sai Rajeswar, Sherjil Ozair, Yoshua Bengio, Aaron Courville, and R. Devon Hjelm. Mutual information neural estimation. In *Proceedings of the 35th International Conference on Machine Learning (ICML)*, pages 531–540, 2018. URL <https://proceedings.mlr.press/v80/belghazi18a.html>.
- Leonard F. Bereska, Zoe Tzifa-Kratira, Reza Samavi, and Efstratios Gavves. Superposition as lossy compression: Measure with sparse autoencoders and connect to adversarial vulnerability. *Transactions on Machine Learning Research (TMLR)*, 2025. URL <https://arxiv.org/abs/2512.13568>. arXiv:2512.13568.
- Yuda Bi, Chenyu Zhang, Qiheng Wang, and Vince D. Calhoun. Grokking as a falsifiable finite-size transition. *arXiv preprint arXiv:2603.24746*, 2026. doi: 10.48550/arXiv.2603.24746. URL <https://arxiv.org/abs/2603.24746>.
- Felix J. Binder, James Chua, Tomek Korbak, Henry Sleight, John Hughes, Robert Long, Ethan Perez, Miles Turpin, and Owain Evans. Looking inward: Language models can learn about themselves by introspection. *arXiv preprint*, arXiv:2410.13787, 2024. doi: 10.48550/arXiv.2410.13787. URL <https://arxiv.org/abs/2410.13787>.
- Jennifer G. Blank, Glenn H. Miller, Mark J. Ahrens, and Randall E. Winans. Experimental shock chemistry of aqueous amino acid solutions and the cometary delivery of prebiotic compounds. *Origins of Life and Evolution of Biospheres*, 31:15–51, 2001. doi: 10.1023/A:1006758803255.
- Daniel M. Busiello, Shiling Liang, Francesco Piazza, and Paolo De Los Rios. Dissipation-driven selection of states in non-equilibrium chemical networks. *Communications Chemistry*, 4:16, 2021. doi: 10.1038/s42004-021-00454-w.
- Stephen Casper, Xander Davies, Claudia Shi, Thomas Krendl Gilbert, Jérémy Scheurer, Javier Rando, Rachel Freedman, Tomasz Korbak, David Lindner, Pedro Freire, Tony Wang, Samuel Marks, Charbel-Raphaël Segerie, Micah Carroll, Andi Peng, Phillip Christoffersen, Mehul Damani, Stewart Slocum, Usman Anwar, Anand Siththaranjan, Max Nadeau, Eric J. Michaud, Jacob Pfau, Dmitrii Krasheninnikov, Xin Chen, Lauro Langosco, Peter Hase, Erdem Bıyık, Anca Dragan, David Krueger, Dorsa Sadigh, and Dylan Hadfield-Menell. Open problems and fundamental limitations of reinforcement learning from human feedback. *Transactions on Machine Learning Research (TMLR)*, 2023. URL <https://openreview.net/forum?id=bx24KpJ4Eb>. Preprint: arXiv:2307.15217.
- Bogdan Chornomaz, Yonatan Koren, Shay Moran, and Tom Waknine. Agnostic learning under targeted poisoning: Optimal rates and the role of randomness. *arXiv preprint*, arXiv:2506.03075, 2025. doi: 10.48550/arXiv.2506.03075. URL <https://arxiv.org/abs/2506.03075>.
- Kenzo Clauw, Sebastiano Stramaglia, and Daniele Marinazzo. Information-theoretic progress measures reveal grokking is an emergent phase transition. *arXiv preprint*, arXiv:2408.08944, 2024. doi: 10.48550/arXiv.2408.08944. URL <https://arxiv.org/abs/2408.08944>.
- Hoagy Cunningham, Aidan Ewart, Logan Riggs, Robert Huben, and Lee Sharkey. Sparse autoencoders find highly interpretable features in language models. *arXiv preprint*, arXiv:2309.08600, 2023. doi: 10.48550/arXiv.2309.08600. URL <https://arxiv.org/abs/2309.08600>.
- Bruce Damer and David Deamer. The hot spring hypothesis for an origin of life. *Astrobiology*, 20(4):429–452, 2020. doi: 10.1089/ast.2019.2045.
- Branton DeMoss, Silvia Sapura, Jakob Foerster, Nick Hawes, and Ingmar Posner. The complexity dynamics of grokking. *Physica D: Nonlinear Phenomena*, 482:134859, 2025. doi: 10.1016/j.physd.2025.134859. Preprint: arXiv:2412.09810.

- Ilias Diakonikolas and Daniel M. Kane. *Algorithmic High-Dimensional Robust Statistics*. Cambridge University Press, 2023. doi: 10.1017/9781108943161.
- David L. Donoho and Peter J. Huber. The notion of breakdown point. In P. J. Bickel, K. Doksum, and J. L. Hodges, editors, *A Festschrift for Erich L. Lehmann*, pages 157–184. Wadsworth, 1983.
- Astrid Eichhorn, David Mesterházy, and Michael M. Scherer. Universal behavior of coupled order parameters below three dimensions. *Physical Review E*, 88:042141, 2013. doi: 10.1103/PhysRevE.88.042141. arXiv:1606.07449 v2 (2017).
- Jeremy L. England. Dissipative adaptation in driven self-assembly. *Nature Nanotechnology*, 10: 919–923, 2015. doi: 10.1038/nnano.2015.250.
- James P. Ferris, Aubrey R. Hill, Rihe Liu, and Leslie E. Orgel. Synthesis of long prebiotic oligomers on mineral surfaces. *Nature*, 381:59–61, 1996. doi: 10.1038/381059a0.
- Alexander Floroni, Noël Yeh Martín, Thomas Matreux, Laura I. Weise, Sheref S. Mansy, Hannes Mutschler, Christof B. Mast, and Dieter Braun. Membraneless protocell confined by a heat flow. *Nature Physics*, 21:1303–1310, 2025. doi: 10.1038/s41567-025-02935-4.
- Mark I. Freidlin and Alexander D. Wentzell. *Random Perturbations of Dynamical Systems*, volume 260 of *Grundlehren der mathematischen Wissenschaften*. Springer, 1984. doi: 10.1007/978-1-4684-0176-9.
- Karl Friston. The free-energy principle: A unified brain theory? *Nature Reviews Neuroscience*, 11:127–138, 2010. doi: 10.1038/nrn2787.
- Frank R. Hampel. A general qualitative definition of robustness. *Annals of Mathematical Statistics*, 42(6):1887–1896, 1971. doi: 10.1214/aoms/1177693054.
- Steve Hanneke, Amin Karbasi, Mohammad Mahmoodi, Idan Mehalal, and Shay Moran. On optimal learning under targeted data poisoning. In *Advances in Neural Information Processing Systems (NeurIPS)*, 2022. doi: 10.48550/arXiv.2210.02713. URL <https://arxiv.org/abs/2210.02713>.
- Nils Hasselmann, Andreas Sinner, and Peter Kopietz. Two-parameter scaling of correlation functions near continuous phase transitions. *Physical Review E*, 76:040101(R), 2007. doi: 10.1103/PhysRevE.76.040101.
- Max Hennick and Guillaume Corlouer. From density matrices to phase transitions in deep learning: Spectral early warnings and interpretability. *arXiv preprint arXiv:2603.29805*, 2026. doi: 10.48550/arXiv.2603.29805. URL <https://arxiv.org/abs/2603.29805>.
- Jesse Hoogland, George Wang, Matthew Farrugia-Roberts, Liam Carroll, Susan Wei, and Daniel Murfet. Loss landscape degeneracy and stagewise development in transformers. *arXiv preprint, arXiv:2402.02364*, 2024. doi: 10.48550/arXiv.2402.02364. URL <https://arxiv.org/abs/2402.02364>.
- Frank P. Kelly. *Reversibility and Stochastic Networks*. John Wiley & Sons, 1979.
- Alexander Kraskov, Harald Stögbauer, and Peter Grassberger. Estimating mutual information. *Physical Review E*, 69:066138, 2004. doi: 10.1103/PhysRevE.69.066138.
- Keith A. Kvenvolden, James Lawless, Katherine Pering, Etta Peterson, Jose Flores, Cyril Ponnamperuma, Isaac R. Kaplan, and Carleton Moore. Evidence for extraterrestrial amino acids and hydrocarbons in the Murchison meteorite. *Nature*, 228:923–926, 1970. doi: 10.1038/228923a0.

- Lucien Le Cam. *Asymptotic Methods in Statistical Decision Theory*. Springer Series in Statistics. Springer-Verlag, 1986. doi: 10.1007/978-1-4612-4946-7.
- Guillaume Lecué and Matthieu Lerasle. Robust machine learning by median-of-means: Theory and practice. *Annals of Statistics*, 48(2):906–931, 2020. doi: 10.1214/19-AOS1828. arXiv:1711.10306 (2017).
- Harvey Lederman and Kyle Mahowald. Emergent introspection in AI is content-agnostic. *arXiv preprint arXiv:2603.05414*, 2026. doi: 10.48550/arXiv.2603.05414. URL <https://arxiv.org/abs/2603.05414>.
- Michael Levin. Darwin’s agential materials: Evolutionary implications of multiscale competency in developmental biology. *Cellular and Molecular Life Sciences*, 80:142, 2023. doi: 10.1007/s00018-023-04790-z.
- Shiling Liang, Paolo De Los Rios, and Daniel M. Busiello. Thermodynamic bounds on symmetry breaking in linear and catalytic biochemical systems. *Physical Review Letters*, 132:228402, 2024a. doi: 10.1103/PhysRevLett.132.228402.
- Shiling Liang, Paolo De Los Rios, and Daniel M. Busiello. Thermodynamic space of chemical reaction networks. *arXiv preprint*, arXiv:2407.11498, 2024b. doi: 10.48550/arXiv.2407.11498. URL <https://arxiv.org/abs/2407.11498>.
- Jack Lindsey. Emergent introspective awareness in large language models. Transformer Circuits Thread, Anthropic, October 2025. URL <https://transformer-circuits.pub/2025/introspection/index.html>.
- E. H. Linfoot. An informational measure of correlation. *Information and Control*, 1(1):85–89, 1957. doi: 10.1016/S0019-9958(57)90116-X.
- Ziming Liu, Ouail Kitouni, Niklas Nolte, Eric J. Michaud, Max Tegmark, and Mike Williams. Towards understanding grokking: An effective theory of representation learning. In *Advances in Neural Information Processing Systems (NeurIPS)*, 2022. doi: 10.48550/arXiv.2205.10343. URL <https://arxiv.org/abs/2205.10343>.
- Ziming Liu, Ziqian Zhong, and Max Tegmark. Grokking as compression: A nonlinear complexity perspective. *arXiv preprint*, arXiv:2310.05918, 2023. doi: 10.48550/arXiv.2310.05918. URL <https://arxiv.org/abs/2310.05918>.
- Uzay Macar, Li Yang, Atticus Wang, Peter Wallich, Emmanuel Ameisen, and Jack Lindsey. Mechanisms of introspective awareness. *arXiv preprint arXiv:2603.21396*, 2026. doi: 10.48550/arXiv.2603.21396. URL <https://arxiv.org/abs/2603.21396>.
- Thomas Matreux, Paula Aikkila, Bettina Scheu, Dieter Braun, and Christof B. Mast. Heat flows enrich prebiotic building blocks and enhance their reactivity. *Nature*, 628:110–116, 2024. doi: 10.1038/s41586-024-07193-7.
- John Maynard Smith and Eörs Szathmáry. *The Major Transitions in Evolution*. Oxford University Press, 1995. ISBN 978-0198502944.
- Brett A. McGuire. 2021 census of interstellar, circumstellar, extragalactic, protoplanetary disk, and exoplanetary molecules. *Astrophysical Journal Supplement Series*, 259(2):30, 2022. doi: 10.3847/1538-4365/ac2a48.
- Sean P. Meyn and Richard L. Tweedie. Stability of Markovian processes III: Foster–Lyapunov criteria for continuous-time processes. *Advances in Applied Probability*, 25(3):518–548, 1993. doi: 10.2307/1427522.

- Neel Nanda, Lawrence Chan, Tom Lieberum, Jess Smith, and Jacob Steinhardt. Progress measures for grokking via mechanistic interpretability. In *The Eleventh International Conference on Learning Representations (ICLR)*, 2023. doi: 10.48550/arXiv.2301.05217. URL <https://arxiv.org/abs/2301.05217>.
- Yasuhiro Oba, Toshiki Koga, Yoshinori Takano, Nanako O. Ogawa, Naohiko Ohkouchi, Kazunori Sasaki, Hajime Sato, Daniel P. Glavin, Jason P. Dworkin, Hiroshi Naraoka, et al. Uracil in the carbonaceous asteroid (162173) Ryugu. *Nature Communications*, 14:1292, 2023. doi: 10.1038/s41467-023-36904-3.
- Catherine Olsson, Nelson Elhage, Neel Nanda, Nicholas Joseph, Nova DasSarma, Tom Henighan, Ben Mann, Amanda Askell, Yuntao Bai, Anna Chen, Tom Conerly, Dawn Drain, Deep Ganguli, Zac Hatfield-Dodds, Danny Hernandez, Scott Johnston, Andy Jones, Jackson Kernion, Liane Lovitt, Kamal Ndousse, Dario Amodei, Tom Brown, Jack Clark, Jared Kaplan, Sam McCandlish, and Chris Olah. In-context learning and induction heads. *Transformer Circuits Thread, Anthropic*, 2022. URL <https://transformer-circuits.pub/2022/in-context-learning-and-induction-heads/index.html>. Preprint: arXiv:2209.11895.
- Simon Pepin Lehalleur, Jesse Hoogland, Matthew Farrugia-Roberts, Susan Wei, Alexander Gietelink Oldenziel, George Wang, Liam Carroll, and Daniel Murfet. You are what you eat—AI alignment requires understanding how data shapes structure and generalisation. *arXiv preprint*, arXiv:2502.05475, 2025. doi: 10.48550/arXiv.2502.05475. URL <https://arxiv.org/abs/2502.05475>.
- Alethea Power, Yuri Burda, Harri Edwards, Igor Babuschkin, and Vedant Misra. Grokking: Generalization beyond overfitting on small algorithmic datasets. *arXiv preprint*, arXiv:2201.02177, 2022. doi: 10.48550/arXiv.2201.02177. URL <https://arxiv.org/abs/2201.02177>.
- Rithvik Prakki. Active inference for self-organizing multi-LLM systems: A Bayesian thermodynamic approach to adaptation. *arXiv preprint*, arXiv:2412.10425, 2024. doi: 10.48550/arXiv.2412.10425. URL <https://arxiv.org/abs/2412.10425>.
- Vickram N. Premakumar, Michael Vaiana, Florin Pop, Judd Rosenblatt, Diogo Schwerz de Lucena, Kirsten Ziman, and Michael S. A. Graziano. Unexpected benefits of self-modeling in neural systems. *arXiv preprint arXiv:2407.10188*, 2024. doi: 10.48550/arXiv.2407.10188. URL <https://arxiv.org/abs/2407.10188>.
- Mikhail Prokopenko, Paul C. W. Davies, Michael Harré, Marcus G. Heisler, Zdenka Kuncic, Geraint F. Lewis, Ori Livson, Joseph T. Lizier, and Fernando E. Rosas. Biological arrow of time: Emergence of tangled information hierarchies and self-modelling dynamics. *Journal of Physics: Complexity*, 6(1):015006, 2025. doi: 10.1088/2632-072X/ad9cdc.
- Maxwell J. D. Ramstead, Dalton A. R. Sakthivadivel, Conor Heins, Magnus Koudahl, Beren Millidge, Lancelot Da Costa, Brennan Klein, and Karl J. Friston. On Bayesian mechanics: A physics of and by beliefs. *Interface Focus*, 13(3):20220029, 2023. doi: 10.1098/rsfs.2022.0029.
- Saroj K. Rout, Sreekar Wunnava, Miloš Krepl, Giuseppe Cassone, Judit E. Šponer, Christof B. Mast, Matthew W. Powner, and Dieter Braun. Amino acids catalyse RNA formation under ambient alkaline conditions. *Nature Communications*, 16:5193, 2025. doi: 10.1038/s41467-025-60359-3.
- J. Schnakenberg. Network theory of microscopic and macroscopic behavior of master equation systems. *Reviews of Modern Physics*, 48(4):571–585, 1976. doi: 10.1103/RevModPhys.48.571.
- Udo Seifert. Stochastic thermodynamics, fluctuation theorems and molecular machines. *Reports on Progress in Physics*, 75(12):126001, 2012. doi: 10.1088/0034-4885/75/12/126001.

- Jyoti Singh, Benjamin Thoma, Daniel Whitaker, Max Satterly Webley, Yuan Yao, and Matthew W. Powner. Thioester-mediated RNA aminoacylation and peptidyl-RNA synthesis in water. *Nature*, 644:933–944, 2025. doi: 10.1038/s41586-025-09388-y.
- Anna Soligo, Edward Turner, Senthoooran Rajamanoharan, and Neel Nanda. Convergent linear representations of emergent misalignment. *arXiv preprint arXiv:2506.11618*, 2025. doi: 10.48550/arXiv.2506.11618. URL <https://arxiv.org/abs/2506.11618>.
- Anna Soligo, Edward Turner, Mia Taylor, Senthoooran Rajamanoharan, and Neel Nanda. Emergent misalignment is easy, narrow misalignment is hard. *arXiv preprint arXiv:2602.07852*, 2026. doi: 10.48550/arXiv.2602.07852. URL <https://arxiv.org/abs/2602.07852>.
- Siyuan Song, Harvey Lederman, Jennifer Hu, and Kyle Mahowald. Privileged self-access matters for introspection in AI. *arXiv preprint arXiv:2508.14802*, 2025. doi: 10.48550/arXiv.2508.14802. URL <https://arxiv.org/abs/2508.14802>.
- Alexandra Souly et al. Poisoning attacks on LLMs require a near-constant number of poison samples. *arXiv preprint arXiv:2510.07192*, 2025. doi: 10.48550/arXiv.2510.07192. URL <https://arxiv.org/abs/2510.07192>. Anthropic, UK AI Security Institute, Alan Turing Institute.
- Quynh Hoa Truong and Xuan Khanh Truong. Prebiotic selection as a physical process: An information quasi-potential framework for chemical convergence. *bioRxiv*, 2026a. doi: 10.64898/2026.04.21.719958. URL <https://www.biorxiv.org/content/10.64898/2026.04.21.719958v2>. Preprint, version 2.
- Xuan Khanh Truong. Ontological phase transitions in learning systems: When context shifts force representational restructuring. Periodic Table of Concepts, Paper V. SSRN preprint, 2026. URL https://papers.ssrn.com/sol3/papers.cfm?abstract_id=6301678. Working paper, version 7. Available on SSRN.
- Xuan Khanh Truong and Quynh Hoa Truong. Norm-hierarchy transitions in representation learning: When and why neural networks abandon shortcuts. *arXiv preprint arXiv:2603.07323*, 2026b. doi: 10.48550/arXiv.2603.07323. URL <https://arxiv.org/abs/2603.07323>.
- Xuan Khanh Truong, Quynh Hoa Truong, Duc Trung Luu, and Thanh Duc Phan. Why grokking takes so long: A first-principles theory of representational phase transitions. *arXiv preprint arXiv:2603.13331*, 2026. doi: 10.48550/arXiv.2603.13331. URL <https://arxiv.org/abs/2603.13331>.
- Edward Turner, Anna Soligo, Mia Taylor, Senthoooran Rajamanoharan, and Neel Nanda. Model organisms for emergent misalignment. *arXiv preprint arXiv:2506.11613*, 2025. doi: 10.48550/arXiv.2506.11613. URL <https://arxiv.org/abs/2506.11613>.
- Sara Imari Walker and Paul C. W. Davies. The algorithmic origins of life. *Journal of the Royal Society Interface*, 10(79):20120869, 2013. doi: 10.1098/rsif.2012.0869.
- Sumio Watanabe. *Algebraic Geometry and Statistical Learning Theory*. Cambridge Monographs on Applied and Computational Mathematics. Cambridge University Press, 2009. doi: 10.1017/CBO9780511800474.
- Jason Wei, Yi Tay, Rishi Bommasani, Colin Raffel, Barret Zoph, Sebastian Borgeaud, Dani Yogatama, Maarten Bosma, Denny Zhou, Donald Metzler, Ed H. Chi, Tatsunori Hashimoto, Oriol Vinyals, Percy Liang, Jeff Dean, and William Fedus. Emergent abilities of large language models. *Transactions on Machine Learning Research (TMLR)*, 2022. URL <https://openreview.net/forum?id=yzkSU5zdWd>. Preprint: arXiv:2206.07682.